IEEE Access
Multidisciplinary ⋮ Rapid Review ⋮ Open Access Journal

Received 24 November 2023, accepted 15 January 2024, date of publication 24 January 2024, date of current version 1 February 2024.

Digital Object Identifier 10.1109/ACCESS.2024.3357978

RESEARCH ARTICLE

Novel Structure of a Solid Rotary Inverter Sensor for Speed Measurement of Vehicles

FAHEEM JAVED[1], ZAHID ULLAH[2], (Graduate Student Member, IEEE), AND MOHSIN KAMAL[3], (Senior Member, IEEE)

[1]Department of Electrical Engineering, College of Electrical and Mechanical Engineering, National University of Sciences and Technology, Islamabad 04623, Pakistan
[2]Dipartimento di Elettronica, Informazione e Bioingegneria, Politecnico di Milano, 20133 Milan, Italy
[3]School of Electrical Engineering and Computer Science, National University of Sciences and Technology, Islamabad 44000, Pakistan

Corresponding author: Zahid Ullah (zahid.ullah@polimi.it)

ABSTRACT Accurate speed measurement and running records are integral to ensure safety and periodic maintenance of vehicles. This paper presents a novel structure of a solid rotary inverter (DAC) sensor for linear speed measurement of vehicles by eliminating reliance on magnets, coils, armatures, and toothed rings. The electromechanical sensor is exited through the vehicle's DC power from the battery and utilizes a specially designed solid rotary part that is rotated mechanically by the wheel, enabling conversion of the DC into three-phase AC. The frequency of the produced AC voltage is proportional to the rotation speed. The three-phase alternating voltage is then used to run an analog speedometer gauge (a three-phase AC motor) to display the linear speed. The study determines stability analysis and response assessment by modeling a novel electromechanical rotational system and then evaluating its optimal design parameters. Real-time output voltage data from the sensor is acquired using a Rohde & Schwarz RTM 2034 oscilloscope and processed in MATLAB R2022b for frequency analysis. Experimental tests are conducted in a laboratory setting, varying the rotational speed sweep of the sensor from 150 to 450 RPM and translating the results into linear speed. A machine learning regression technique is applied to features such as shaft rotational speed, angular velocity, frequency, and period with linear speed. The obtained results reveal a total harmonic distortion (THD) value of −28.9778 dB (3.557%), meeting the criteria outlined in the IEEE 519-2014 "Recommended Practice and Requirements for Harmonic Control in Electric Power Systems."

INDEX TERMS Solid shaft, speedometer sensor, inverter, system modeling, total harmonic distortion.

I. INTRODUCTION

The instrument panel on the dashboard of a vehicle organizes various indications and gauges including fuel level gauge, water temperature indicator, odometer, speedometer, oil pressure gauge and many more. The most important and prominent among these indications and gauges that require driver attention while driving is the speedometer. Speedometer sensors are fundamental components used in vehicles to provide real-time information about speed. Speeding can lead to various hazardous situations, such as rolling in curvy turns, jack-knifing during braking, or losing control of the vehicle on slippery road surfaces [1]. Road accidents are often linked to misjudgments in speed and are ranked second most among the factors that verdicts the truck driver committed fault [2].

The existing conventional tracked vehicles in Pakistan exhibit outdated features, possessing mechanical systems, and lacking Electronic Control Units (ECUs). This renders conventional speed measurement techniques ineffective, and integrating modern speed sensors into these vehicles is unfeasible. Tracked vehicles are frequently chosen for applications where conventional wheeled mobility is inadequate. Unlike their wheeled counterparts, tracked vehicles encounter a distinct challenge when it comes to converting their rotational movement into conventional speed measurements. This issue becomes especially significant in situations where precise linear speed measurement is essential. These problems can be eliminated by a sensor-less rotary-based three-phase inverter.

The associate editor coordinating the review of this manuscript and approving it for publication was Snehal Gawande.

In this study, our primary focus centers on the design of a rotary active inverter speed sensor, seeking to redefine linear speed measurement by eliminating reliance on armatures, magnets, coils, and toothed gears.

The speed measurement system comprises two main components, which are the vehicle speed sensors (VSS) or wheel speed sensor (WSS) or rotational speed sensors (RSS), for sensing the rotational speed and the analog dial or digital display on the dashboard or driver panel termed the tachometer or speedometer. The primary purpose of sensors is to measure the rotational speed of an automotive gear box, fly wheel, or drive wheel and convert it into an electrical signal that can be interpreted by the speedometer dial or display. Vehicle speed sensors (VSS) can broadly be classified into two categories. Traditional speedometer sensors relied on mechanical systems, such as cables and gears, to transfer the wheel's rotational speed to the speedometer. With advancements in technology, modern vehicles now predominantly use electronic speedometer sensors [3].

Electronic speedometers operate based on the principle of either the hall effect or magnetic induction. In the magnetic induction variant, a gear or toothed ring is affixed to the wheel or shaft, which requires rotational speed measurement. A magnetic coil is positioned adjacent to the gear or ring. As the wheel rotates, it causes the toothed ring to spin along with it, generating a changing magnetic field in the coil. Due to this, an electrical signal is produced whose frequency is correlated to the rotational speed of the shaft. The electrical signal is forwarded to the vehicle's powertrain control module (PCM) or the electronic control unit (ECU). The task of PCM or ECU is to interpret and process these signals and display them in the form of linear speed on the vehicle's dashboard.

In contrast, the Hall effect speedometer sensors, as the name indicates, work on the Hall effect phenomenon. According to this phenomenon, a voltage difference in a semiconductor is produced when it is exposed to a magnetic field. In this configuration, a magnet is fastened to the moving part of the vehicle, while a Hall effect sensor is positioned in proximity. Whenever the magnet passes the sensor during rotation, its magnetic field is disturbed, which results in a variation of the voltage in the sensor. The fluctuation in the voltage is captured and translated into a digital signal. This signal is subsequently utilized to ascertain the speed of the wheel and is finally visualized on the speedometer.

In the realm of modern power electronics, the DC to AC converter, commonly referred to as an inverter, stands as a cornerstone technology that facilitates the seamless interconnection between direct current (DC) sources and alternating current (AC) grids. Its significance amplifies across a wide spectrum of applications, not limited to motors running, renewable energy integration, electric vehicle propulsion, uninterruptible power supplies, industrial automation, and more.

The integration of a solid rotary DC to AC inverter offers a novel avenue to address this issue, seamlessly fusing the principles of electrical engineering and mechanical dynamics. This study explores the utilization of DC to AC inverters acting as a vehicle speed sensor (VSS) for measuring the linear speed of tracked vehicles. By exploiting the inverter's transforming capabilities, this research endeavors to bridge the gap between rotational motion and measurable linear speed, enhancing the overall operational understanding and performance evaluation of tracked vehicles.

II. RELATED WORK

A vehicle's driver most often periodically glimpses the speedometer for various purposes while driving: to adhere speed limits, keep the speed within safety margins, perform accelerometer adjustments in circumstances that necessitate speed monitoring [4]. Literature reveals that accurate speed measurement is an active area of research, and various methodologies have been published in this field of research. Singh and Porwal [5] employed the conversion of analog dial speed readings into digital numeric display using image processing, enabling quick speed checks and minimizing the need to divert attention from the road. A digital speedometer is implemented on FPGA; obtaining pulse information from a hall sensor is proposed in [6]. Digital image processing techniques are used to measure rotation motion in [7]. The basic phenomenon of linear speed measurement relies on the measurement of rotational speed measurement of the wheel, transmission gear or a solid shaft on board the vehicle. An experimental tool is implemented and tested in [8] to convert angular velocity into linear velocity based on Arduino ATMega 2560. Reference [9] assumed the universe to be spherical in shape and tried to calculate rotational and linear speed of the universe. A speed sensor is introduced in [10] that employs the fluxgate effect within an amorphous ring core to detect the field generated by motional eddy currents. The work presented in [11] and [12] demonstrated linear speed measurements for solid conductive objects utilizing eddy current speed sensors. An eddy current speed sensor composed of an excitation coil and pick-up coil placed perpendicular to each other around a sold shaft is presented in [13]. A voltage is induced in the pick-up coil as the shaft rotates due to changes in net magnetic flux the pick-up coil. The induced voltage is directly proportional to the rotational speed of the shaft. In contrast to variable reluctance and optical speed sensors, as well as tachometers and resolvers, the suggested eddy current speed sensor operates without the need for any supplementary components or gears to be affixed to the rotating shaft. An eddy current speed sensor composed of a single excitation coil and two pick-up coils for rotating rods and cylindrical shafts is also presented in [14]

A novel non-contact approach to measure rotational speed using electrostatic sensors is proposed in [15]. The percentage error was high at lower RPMs. Four electrostatic sensors are placed at right angle to each other, with the rotating shaft in between these sensors. An electrostatic charge develops on the surface of the rotating solid shaft because of the air friction. Due to the electrostatic induction principle, the

sensors can sense any movement of the surface, and the speed of rotation can be determined based on the similarity of the signals from the four sensors. An auto-correlation technique is applied to find a time delay between two signals to calculate the speed, however, the accuracy of this technique is affected by the sampling rate and signal noise [16]. I. [17] proposed three different algorithms using a digital wave implementation of an electrostatic sensor that generates a square pulse every rotation period, hence determining the rotation speed. At low speed, the amount of charge on the strip is unstable, hence, the response time is poor. A methodology to measure vehicle speed using magneto resistive vehicle detection equipment buried in road is introduced in [18].

III. PROPOSED METHODOLOGY

The conventional speed sensors are based on magnets, coils, windings or the toothed ring to measure the speed. Signal from these sensors is obtained in digital form or pulse shape for further processing. Tracked vehicles lacking ECUs to process digital signals necessitate an alternate approach to measure the speed. This paper introduces a novel approach to powering the three-phase motor inside speedometer in tracked vehicles, employing a solid rotary DC-to-AC converter and eliminating reliance on magnets, coils and toothed rings. The converter provides the necessary AC current by converting the available 24V DC power from the vehicle's electrical system. The speedometer is based on the design of the DC tachogenerator, which consists of a rotary and a stationary circuit instead of a permanent magnet. The design incorporates carbon brushes as the source of input and output for the system.

A. WORKING PRINCIPLE

The solid rotary DC-to-AC converter consists of a mechanical assembly where a solid rotary part is connected to the rotating wheel of the tracked vehicle. The rotary part is divided into three sections, each playing a specific role in the conversion process. Two of the sections remain in constant contact with the 24 VDC input for the vehicle electrical system and the ground, respectively, through brushes. These brushes ensure a reliable electrical connection to maintain a steady power supply. The middle section of the rotary is connected to three additional brushes placed at 120 degrees to each other that enable the switching of the current, resulting in the generation of a three-phase AC output. A schematic diagram of the system is shown in Fig. 1.

B. DESIGN AND CONSTRUCTION OF THE PROPOSED SOLID ROTARY SENSOR

1) SOLID ROTARY

A solid rotary is a cylindrical-shaped rotor. The two ends of the rotor are copper conductors that are electrically insulated from each other. The insulated section is in between the two conductors and made of solid fiber. The fiber insulation is plastered on a steel rod to keep the copper conductors in fixed

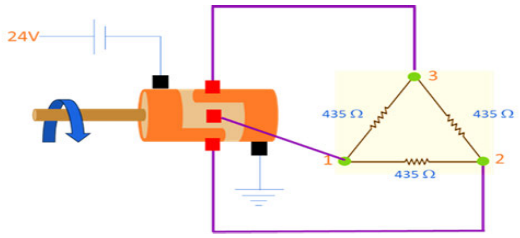

FIGURE 1. Proposed layout of the solid rotary inverter speed sensor.

position and ensure reliable rotation of the rotor, as shown in Fig. 2.

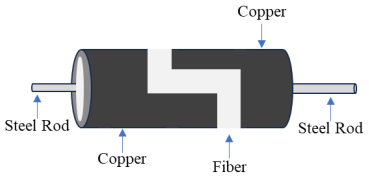

FIGURE 2. Construction of solid rotary shaft.

2) THE STATOR OR THE CONNECTION DESIGN AND CONSTRUCTION

Main layout of the sensor is illustrated in Fig. 3. The solid rotor is placed in a center position between the slots made in three fiber plates. Each of the fiber plates has carbon brushes fixed to it. The fiber plate ensures electrical insulation and serves as fixture for the carbon brushes, so that a reliable electrical connection is ensured between the rotor surface and the brushes. The fiber plates are fixed using copper plates at an appropriate distance, so the front, middle and back ends are at exact locations where the carbon brushes maintain a reliable connection with the rotor. The copper plates also serve as conductor of current to and from the carbon brushes. The front shaft is connected to the wheel for effective rotation.

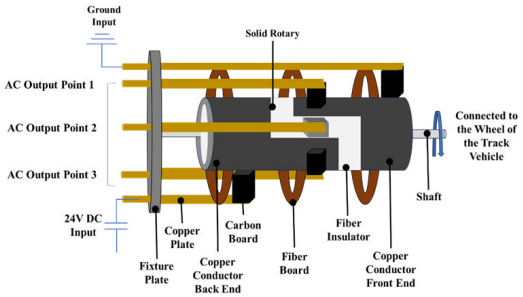

FIGURE 3. Proposed layout of the rotary inverter sensor.

C. SPEEDOMETER GAUGE CONSTRUCTION

The speedometer analogue gauge is a moving pointer display type. It comprises of a AC Synchronous Unexcited Hysteresis three phase motor, speed cup, torsion spring, needle and a dial

gauge with evenly spaced markings. The primary components of the motor consist of the stator and rotor. The stator features three-phase windings positioned at 120-degree intervals from one another. The rotor is a cylindrical magnet affixed to the shaft's center. This shaft is free to rotate due to the presence of bearings fixed at both its upper and lower ends. At the top of the shaft is the speed cup which has a cut at the top surface. The speed cup has the pointer needle fixed at its top center. In between the speed cup and needle is placed the equally spaced numbered dial gauge. The pointer is fixed to zero position through the torsion spring.

1) CURRENT SWITCHING MECHANISM

The shaft of the solid rotary of the DC to AC converter is connected to the wheel of the track vehicle to measure its linear speed through the conversion of rotary speed into a linear value. As the wheel rotates, it causes the rotary shaft to rotate at the same rotational speed and frequency as that of the wheel. Two inputs are provided to the system, i.e., 24V DC and ground. As shown in Fig. 3, the front copper metal of the rotor is connected to the ground, and the tail end (bottom copper metal) is connected to the input DC voltage. The switching functionality within the solid rotary converter is accomplished through the three brushes connected to the middle section of the rotary. As the solid rotary rotates due to the spinning of the wheel, it selectively connects and disconnects these brushes. The converter effectively alternates the current flow, producing a 3-phase AC waveform. Consider the AC output at point 1, as the rotor spins, this point at an instant will be connected to the ground; at the next moment, it will contact the fiber insulator, and furthermore, it will connect to the input DC power. In this manner, as the rotor continues spinning, this process will continue. The continuous break of the DC will result in AC power generation. The timing and coordination of the switching mechanism are critical to ensure the accuracy and stability of the generated AC current. The magnitude of the generated AC voltage through the switching mechanism is proportional to the rotation speed.

2) SPEEDOMETER OPERATION

The DC-to-AC inverter produces three-phase AC power to run the AC motor within the speedometer. The speedometer is made of a specially designed AC motor with a cup-speed analog dial gauge. The rotational speed of the track vehicle's wheel is transformed into linear speed as presented on the analog speedometer dial gauge. The needle on the cup deflects to display the linear speed on an equally distributed scale. When the vehicle is stationary, the wheel does not rotate. No AC current is generated. The speedcup is fixed to a zero point by a coil spring in the absence of any external force. The AC power generated by the inverter is further utilized to drive the AC motor in the speedometer. The motor exerts torque on the cup to spin it in the direction of the exerted force. The amount of torque corresponds to the induced rotational force. This force causes the needle attached to the speed cup to deflect in the direction of the exerted torque. The exerted torque is balanced by a torsion spring, attached to the speed cup. The amount of deflection is proportional to the exerted torque. The generated force can be calibrated through the meticulous use of delta-configured resistors and gears, so that a calibrated force is generated to deflect the dial to accurate linear speed in kilometers per hour on the speedometer.

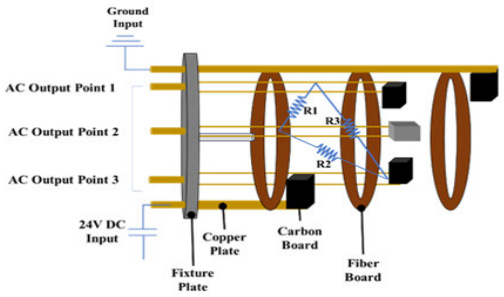

FIGURE 4. Current limiter circuit.

D. SYSTEM MODELING

The proposed sensor is considered an electromechanical rotational system. Free body diagram of the sensor is shown in Fig. 5.

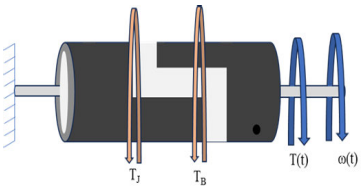

FIGURE 5. Free body diagram of proposed sensor model.

D'Alembert's principle introduced a concept known as ''virtual work'', according to which the net torques acting on a body equal zero. Mathematically,

$$T(t) = T_J + T_B = \frac{dw}{dt} + Bw \tag{1}$$

where ''w'' is the angular velocity of the solid shaft, T_J is the resistance torque due to moment of inertia and T_B is the damping friction. T(t) is the torque applied to the shaft by the wheel of the vehicle. Applying Laplace Transform on (1), we get

$$T(s) = sJw(s) + Bw(s) \tag{2}$$

The transfer function from (2) is obtained as under,

$$\frac{w(s)}{T(s)} = \frac{1}{sJ + B} \tag{3}$$

The output being analyzed is the voltage from the sensor, the generated output voltage depends on the angular velocity of the solid shaft. Putting

$$V(t) = k * w(t) \tag{4}$$

Alternatively, we can write (4) as

$$w(t) = \frac{V(t)}{k} \tag{5}$$

Putting (5) in (3), we get

$$\frac{V(s)}{T(s)} = \frac{k}{sJ + B} \tag{6}$$

Equation (6) is the transfer function of the electromechanical system. However, the standard from of first-order differential function and transfer function, respectively, are as under:

$$T(t) = T\frac{dy(t)}{dt} + y(t) \tag{7}$$

$$G(s) = \frac{k}{s/T + 1} \tag{8}$$

The transfer function in standard form can be written as follows:

$$\frac{V(s)}{T(s)} = \frac{k/B}{s(J/B) + 1} \tag{9}$$

where J/B is the time constant (T), the lower the value, the better the system's response.

E. MOMENT OF INERTIA (J)

The moment of inertia of a disk or cylinder depends on the radius. Hence, the net moment of inertia is the sum of the moment of inertia of all the radii of the shaft shown in Fig. 6. The methodology to determine the moment of inertia of a disk or a solid shaft is described in Fig. 7.

$$NetJ = \frac{1}{2}(m_1r_1 + m_2r_2 + m_3r_3) \tag{10}$$

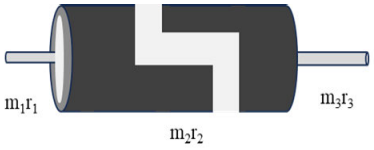

FIGURE 6. Dimensions of the solid shaft for moment of inertia.

F. DAMPING COEFFICIENT (B)

The damping friction values are standardized by the research community between particular surfaces, the values are shown in Table. 1 for the materials used in this study.

TABLE 1. Damping friction values.

Material1	Material2	Static Friction	Sliding Friction
Copper	Cast Iron	1.05	0.29
Copper	Glass	0.68	0.53
Copper	Steel	0.53	0.36
BACF	Steel	0.53	61.64
Carbon	Steel	0.11-0.14	-

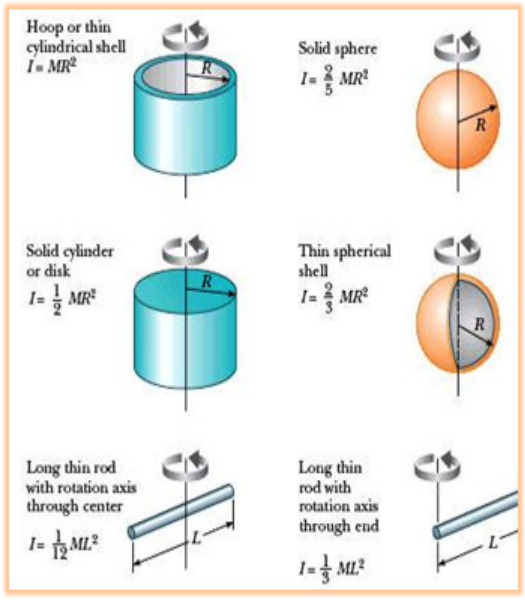

FIGURE 7. Methodology to calculate moment of inertia of a disk or shaft.

The step response of the proposed model is calculated as under:

$$T(s) = \frac{k}{sJ + B)} = \frac{k/J}{(s + (B/J))} \tag{11}$$

$$C(s) = \frac{A}{s}\frac{k}{(sJ + B)} \tag{12}$$

After partial fraction we obtain

$$C(s) = \frac{Ak}{Bs} - \frac{Ak}{(B(s + B/J))} \tag{13}$$

The Inverse Fourier Transform (IFT) of the system is as under:

$$c(t) = \frac{Ak}{s}\frac{1}{(sJ + B)} \tag{14}$$

After partial fraction, we obtain

$$c(t) = \frac{Ak}{B(1 - e^{(} - B/Jt))} \tag{15}$$

The critical parameters of the proposed model are evaluated in MATLAB R2022b, we get the response as shown in Fig. 7.

The system's response is investigated across three distinct damping friction values, while maintaining a constant moment of inertia and disregarding the resistance introduced by carbon brushes. The time constant (T) exhibits an inverse relationship with the damping coefficient, prompting a systematic variation of the damping coefficient to identify an optimal time constant value. Notably, the optimal time constant (T) is attained with a damping coefficient of 1.05.

The stability analysis of the proposed model is conducted through the examination of Bode and Nyquist plots. The Bode plot illustrates a behavior akin to that of a low-pass filter, with the system remaining in phase at lower frequencies.

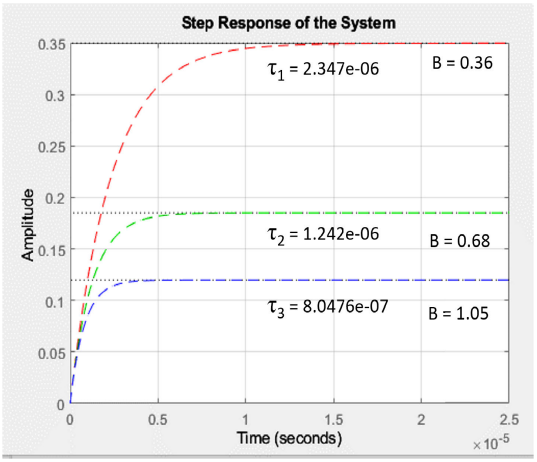

FIGURE 8. Response of the system to step input.

The model's stability is corroborated by the absence of a frequency at −180° phase. At higher frequencies, where the gain reaches a minimum, the Nyquist plots converge towards the origin. The absence of gain values at −180° phase signifies a stable system response, as visually represented in Fig. 8. This comprehensive investigation into the system's response and stability characteristics contributes valuable insights into the dynamic behavior of the proposed model under varying damping coefficients.

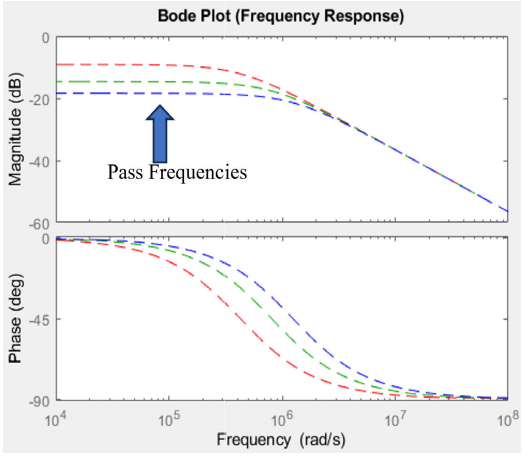

FIGURE 9. Bode plot.

IV. RESULTS AND FINDINGS

The experiments are conducted in laboratory setup under ambient temperature and humidity conditions as illustrated in Fig. 9. The solid rotary sensor is rotated by fixing a battery-operated drill machine to the shaft front end. The RPM of the shaft is obtained using an optical tachometer. The rotational speed, measured in RPM (revolutions per minute), was determined using an optical tachometer connected to the shaft. The sensor received a stable 24 VDC power supply from an external source. A 5-strand cable facilitated the transmission of DC voltage to the sensor, while the remaining three strands were utilized to obtain the three-phase AC output voltage. The output voltage is also provided to the speedometer gauge to show the speed in kmph as shown in Fig. 11.

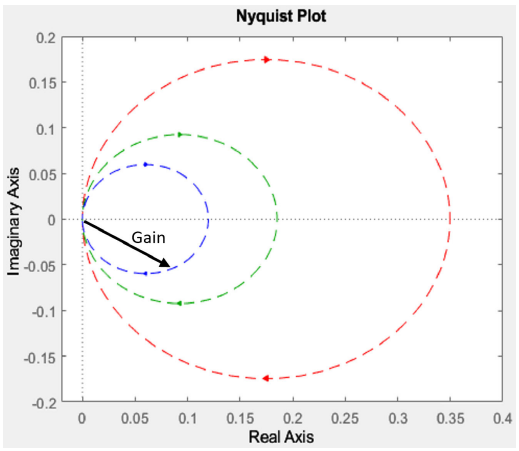

FIGURE 10. Nyquist plot.

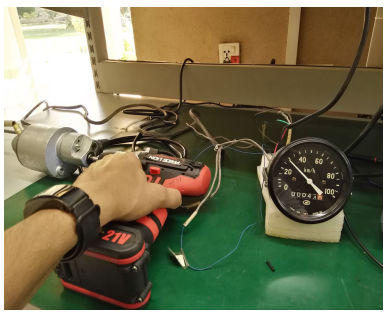

FIGURE 11. Displaying linear speed on the speedometer gauge.

The three-phase output was subsequently linked to a speedometer gauge, which played a crucial role in converting the rotary speed information (in RPM) into linear speed (in kmph). Real-time data from the sensor's output voltage was acquired using a Rohde & Schwarz RTM 2034 oscilloscope. The integration of a battery-operated drill, optical tachometer, power supply, and oscilloscope in this system facilitated a comprehensive analysis of the sensor's performance in translating rotary motion into usable linear speed data.

The output signal of the sensor is obtained on the oscilloscope, as shown in Fig. 12 and the data is saved on USB for porting to laptop and MATLAB R2022b for further analysis. The sampling frequency of the oscilloscope is set to 19998 Hz. The three-phase output signal is plotted in MATLAB separately as well as together for better comparison, as illustrated in Fig. 14 and 15. Since the carbon brushes are placed at 120 degrees to each other in a circular fashion, similar results are obtained in MATLAB where the three phases are at 118.88°, 119.36° and 123.48°, approximately 120° degrees. The DC offset values for each phase are found to be 1.16V, 1.17V and 1.20V, respectively,

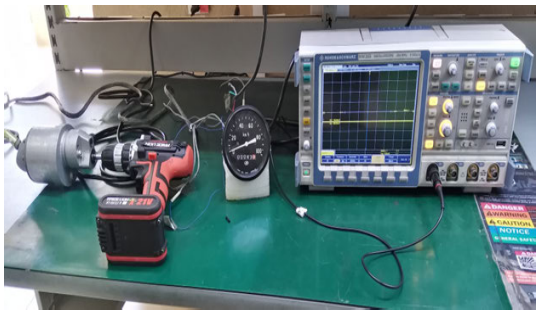

FIGURE 12. Experimental tests of the proposed sensor.

as depicted in Fig. 15. The fundamental frequency is obtained at around 8 Hz and period of 0.12 sec. Fast Fourier Transform of the output voltage reveals harmonics at lower frequencies in the sinusoidal signal, depicted in Fig. 16 and 17. Total harmonic distortion (THD) analysis of the signal shape was carried out and found to be −14.4130 dB which is equivalent to 19.026% (displayed in Fig. 18). Results of the work after application of a low-pass butter work filter to the original signal greatly improved the THD value to −28.9778 dB, equal to 3.557% (displayed in Fig. 19). The results that qualify the acceptable limits of total harmonic distortion in electrical systems have been standardized vide IEEE 519-2014 "Recommended Practice and Requirements for Harmonic Control in Electric Power Systems".

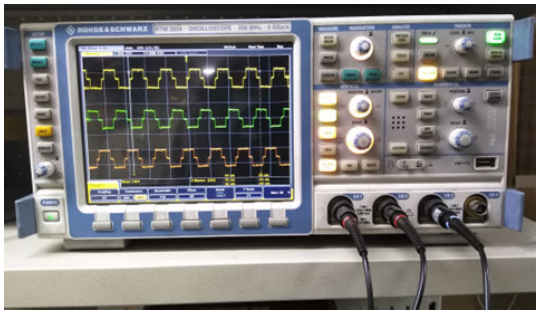

FIGURE 13. Phase wise AC voltage signal from the sensor.

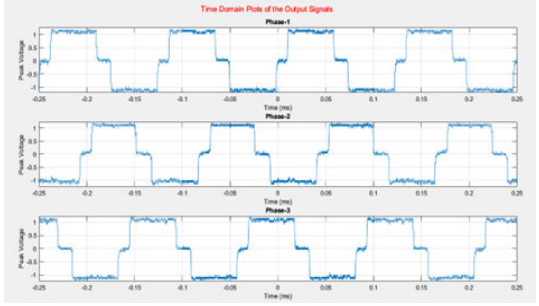

FIGURE 14. Phase wise plot of the voltage signal in MATLAB.

The relationship of solid shaft rpm to the output speed is obtained using machine learning (ML) linear regression

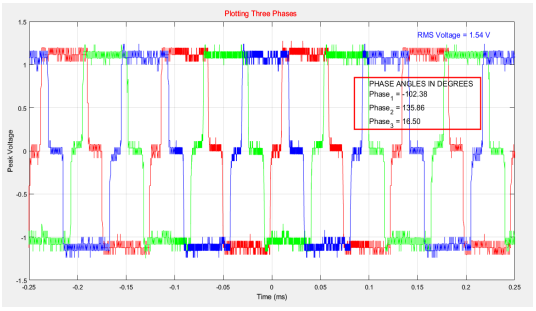

FIGURE 15. Plot of the three phases together in MATLAB.

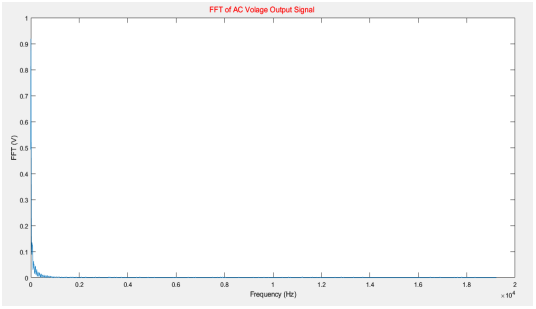

FIGURE 16. FFT of the first phase of the signal.

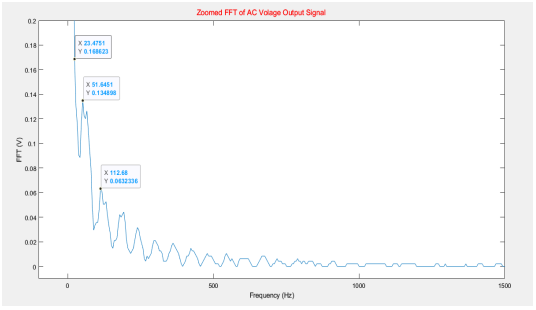

FIGURE 17. Zoomed plot of the FFT of the first phase of the signal.

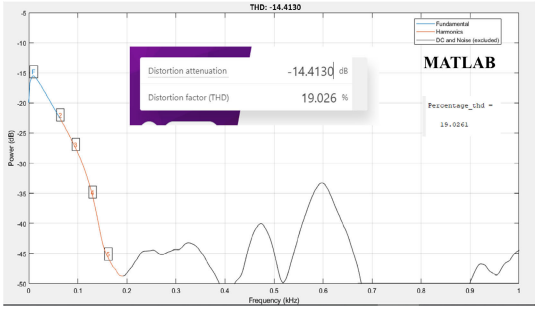

FIGURE 18. THD analysis of the original signal from sensor.

technique. The rotational speed of the sold shaft is obtained using optical tachometer. The rpm value is converted into angular velocity using following equation,

$$w = RPM * 2 * \frac{pi}{60} \tag{16}$$

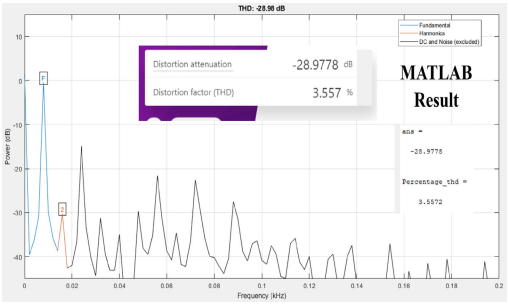

FIGURE 19. THD analysis of the signal after low pass filter.

TABLE 2. Machine learning data for optimization algorithm).

RPM (rev/min)	Ang Vel (rad/sec)	Frequency (Hz)	Period (msec)	Speed (Kmph)
150	15.70796	3.01	332	15
187	19.48259	3.62	275	20
263	27.54129	5.15	195	30
300	31.41592	5.96	167	35
363	38.01327	6.47	154	39
425	44.50589	8.06	124	49

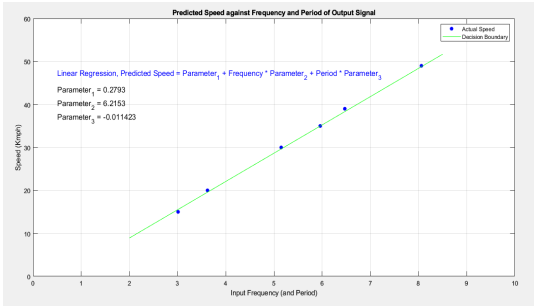

FIGURE 20. Linear regression best fit curve obtained using ML technique.

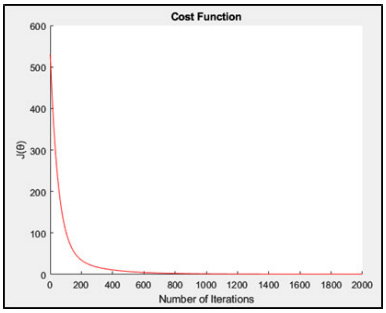

FIGURE 21. Cost function plot optimization with 2000 iterations.

The frequency and period information of the output AC voltage for a single phase (as all the phases deliver similar behaviour) correlated to different sweeps of rotational speed between 150 to 450 rev/ min. The collected sample of data is displayed in table 2.

Machine learning regression optimization algorithm is applied to the collected data. Linear as well as non-linear functions were applied to the data to find the best estimation of the actual linear speed. Optimal parameters were obtained using the training data mentioned in table 2. The parameters were fed in the linear function in (17) for prediction. Results

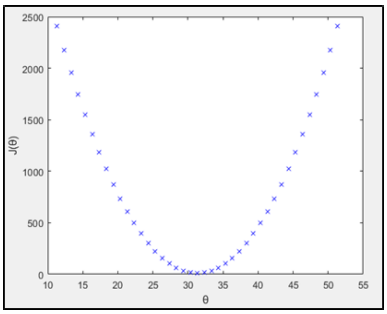

FIGURE 22. ML parameter optimization to find global minima.

indicate a linear relationship between the frequency and period information of the output signal and the linear speed in kmph as obtained using the formula mentioned below, as depicted in Fig. 20. The blue dots in the curve represent the actual speed displayed on the speedometer gauge, while the green line is the best ideal fit obtained using linear regression. The cost function optimization curve and the global minima optimization curve are shown in Fig. 21 and 22.

$$Predictedspeed(kmph) = P_1 + freq * P_2 + period * P_3 \tag{17}$$

where P_i are the parameters of the algorithm.

V. CONCLUSION

The study demonstrated successful implementation of a robust solid rotary electromechanical control system, exhibiting a response profile akin to that of a low-pass filter. The frequency analysis of the inverter output data revealed efficient application of the proposed rotary mechanism for linear speed measurement. The total harmonic distortion values exhibited by the sensor remained well within the acceptable limits defined by IEEE standards. Results indicate a linear relationship between the output voltage information and the observed linear speed in a laboratory setting, making the study best suited for measuring the linear speeds of tracked vehicles lacking ECUs and digital signal processing capabilities. A value addition to the research may be done in the case of utilizing better-conducting-quality metals other than copper and an insulation material other than fiber. The output response of the proposed sensor model may be evaluated at different radii of the shaft.

REFERENCES

[1] M. Francois, F. Osiurak, A. Fort, P. Crave, and J. Navarro, "Analogue versus digital speedometer: Effects on distraction and usability for truck driving," in *Proc. Eur. Conf. Hum. Centred Design Intell. Transp. Systems*, 2016, p. 8.
[2] V. Trucks, "European accident research and safety report 2MI3," Volvo Trucks, Gothenburg, Sweden, Tech. Rep. 2013, 2013.
[3] A. Muir. *How a Speedometer Works*. Accessed: Sep. 21, 2023. [Online]. Available: https://www.howacarworks.com/accessories/how-a-speedo-works/
[4] E. Lehtonen, N. Malhotra, N. J. Starkey, and S. G. Charlton, "Speedometer monitoring when driving with a speed warning system," *Eur. Transp. Res. Rev.*, vol. 12, no. 1, pp. 1–12, Dec. 2020.

[5] S. Singh and Y. Porwal, "An approach to implement analog-to-digital conversion of speedometer using vision," *Int. Res. J. Modernization Eng. Technol. Sci.*, vol. 2, no. 5, 2020.
[6] A. Adhikary, S. Saha, and R. Sarker, "Real time design & implementation of digital speedometer on FPGA," *Int. J. Innov. Res. Develop.*, vol. 2, no. 6, 2013.
[7] X. Zhang, J. Chen, Z. Wang, N. Zhan, and R. Wang, "Digital image correlation using ring template and quadrilateral element for large rotation measurement," *Opt. Lasers Eng.*, vol. 50, no. 7, pp. 922–928, Jul. 2012.
[8] E. Sesa, A. Feriyono, M. Djamal, M. D. T. Musa, M. S. Ulum, and D. Farhamsa, "The design and implementation of an instrument for converting angular velocity to linear velocity based on Arduino ATMega 2560," *J. Phys., Conf. Ser.*, vol. 1434, no. 1, Jan. 2020, Art. no. 012001.
[9] G. Saleh, "The real linear and rotational velocity of the universe and its radius," in *Proc. Int. Annu. Meeting German Astronomical Soc. (AG Meeting)*, 2022, p. 119.
[10] T. Sonoda, R. Ueda, K. Fujitani, T. Irisa, and S. Tatata, "DC magnetic field type eddy current speed sensor detecting cross magnetization field with amorphous core," *IEEE Trans. Magn.*, vol. MAG-21, no. 5, pp. 1732–1734, Sep. 1985.
[11] N. Takehira, A. Tanaka, and K. Toda, "Analysis of a speed-meter utilizing eddy current effect," *Trans. Inst. Electr. Eng. Jpn. A*, vol. 97, no. 9, pp. 457–464, 1977.
[12] M. Mirzaei, P. Ripka, and V. Grim, "A novel eddy current speed sensor with a ferrite E-core," *IEEE Magn. Lett.*, vol. 11, pp. 1–5, 2020.
[13] M. Mirzaei, P. Ripka, and V. Grim, "A novel structure of an eddy current sensor for speed measurement of rotating shafts," *IEEE Trans. Energy Convers.*, vol. 38, no. 1, pp. 170–179, Mar. 2023.
[14] M. Mirzaei, P. Ripka, V. Grim, and A. Chirtsov, "Design and optimization of an eddy current speed sensor for rotating rods," *IEEE Sensors J.*, vol. 20, no. 20, pp. 12241–12251, Oct. 2020.
[15] L. Wang, Y. Yan, Y. Hu, and X. Qian, "Rotational speed measurement through electrostatic sensing and correlation signal processing," *IEEE Trans. Instrum. Meas.*, vol. 63, no. 5, pp. 1190–1199, May 2014.
[16] L. Li, X. Wang, H. Hu, and X. Liu, "Use of double correlation techniques for the improvement of rotation speed measurement based on electrostatic sensors," *Meas. Sci. Technol.*, vol. 27, no. 2, Feb. 2016, Art. no. 025004.
[17] L. Li, H. Hu, Y. Qin, and K. Tang, "Digital approach to rotational speed measurement using an electrostatic sensor," *Sensors*, vol. 19, no. 11, p. 2540, Jun. 2019.
[18] W. Zhang, L. Wang, C. Li, M. Chen, and S. Tao, "Research on vehicle speed detection technology based on micro-magnetoresistive sensing equipment," in *Proc. MATEC Web Conf.*, vol. 139, 2017, p. 208.

FAHEEM JAVED received the bachelor's degree in computer system engineering from the Department of Computer Engineering, College of Electrical and Mechanical Engineering, National University of Sciences and Technology (NUST), Islamabad, Pakistan, in 2009. He is currently pursuing the M.S. degree in electrical engineering with the Department of Electrical Engineering, College of Electrical and Mechanical Engineering, NUST.

ZAHID ULLAH (Graduate Student Member, IEEE) received the B.S. degree in electrical engineering from UET Peshawar, in 2014, and the M.S. degree in electrical engineering from COMSATS University Islamabad, Abbottabad Campus, Abbottabad, Pakistan, in 2017. He is currently pursuing the Ph.D. degree in electrical engineering with Politecnico di Milano, Italy. He was a Lecturer with UMT, Lahore, Pakistan, from 2017 to 2020. He has published various papers in reputed journals and IEEE conference proceedings. His research interests include smart grid, energy management, renewable energy systems, ICTs for power systems, V2G, and machine and deep learning.

MOHSIN KAMAL (Senior Member, IEEE) received the M.S. degree in electrical engineering from the Blekinge Institute of Technology, Karlskrona, Sweden, in 2012, and the Ph.D. degree in electrical engineering from the National University of Computer and Emerging Sciences (FAST-NUCES), Pakistan, in 2020. He completed his Postdoc from the KIOS Research and Innovation Center of Excellence, University of Cyprus, in 2022, under the supervision of Prof. Georgios Ellinas. From March 2013 to February 2021, he was an Assistant Professor with FAST-NUCES. From February 2022 to August 2022, he was the In-Charge of the Electrical Engineering Department, FAST-NUCES, Peshawar Campus. He is currently an Associate Professor with the School of Electrical Engineering and Computer Science (SEECS), National University of Sciences and Technology (NUST). Previously, he was an Associate Professor with the Department of Electrical Engineering, FAST-NUCES, Lahore Campus. He is a Ph.D. approved Supervisor and has supervised the M.S. and B.S. students for their thesis and final year projects, respectively. His research interests include the development of lightweight solutions for various IoT applications, cyber physical systems, blockchain, cyber security, wireless sensor networks, cooperative communication, and cognitive radio networks. He is a reviewer of many renowned Q1 journals and also serves as a technical program committee (TPC) member for national and international conferences.

Open Access funding provided by 'Politecnico di Milano' within the CRUI CARE Agreement